Molecular Therapy
Nucleic Acids
Original Article

Shrimp miR-34 from Shrimp Stress Response to Virus Infection Suppresses Tumorigenesis of Breast Cancer

Yalei Cui,[1] Xiaoyuan Yang,[1] and Xiaobo Zhang[1]

[1]College of Life Sciences and Laboratory for Marine Biology and Biotechnology of Qingdao National Laboratory for Marine Science and Technology, Zhejiang University, Hangzhou 310058, The People's Republic of China

During host stress response against virus infection, some animal microRNAs (miRNAs) can be upregulated to restore the virus-caused metabolic disorder of host cells via suppressing the expressions of miRNAs' target genes. These antiviral miRNAs may have antitumor capacity, because tumorigenesis results from metabolic disorder of cells. However, this subject has not been explored. In this study, the results showed that shrimp miR-34, which was upregulated during white spot syndrome virus (WSSV) infection, had antiviral activity in shrimp. The expression of shrimp miR-34 in breast cancer cells and in mice suppressed the growth and metastasis of breast cancer by targeting human *CCND1*, *CDK6*, *CCNE2*, *E2F3*, *FOSL1*, and *MET* genes in a cross-phylum manner. The results of this study indicated that miRNAs with antiviral activities can be promising sources for antitumor drug discovery.

INTRODUCTION

Stress broadly refers to living cells being suddenly challenged by conditions of a strong and harmful stimulus, such as trauma, surgery, infection, or hypoxia. Reports have shown that stress can be caused by infection of a variety of viruses.[1,2] Infection of human monocyte-macrophages by vaccinia virus induces a severe stress response, leading to significant decreases of mRNA expression levels and activation of interactions between heat shock proteins and viral components.[1] Newcastle disease virus infection can stimulate the stress response and accumulate the mRNAs and proteins in cells.[2] Once cells are exposed to conditions of environmental stress, the cells would deviate from the original status, resulting in abnormality of macromolecules (proteins, mRNAs, DNAs, and lipids) and even causing metabolic imbalance.[3] To adapt to the external environment and survive from the injuries, the cells have evolved multiple mechanisms to deal with different stress responses, such as clearance of damaged macromolecules by autophagy,[4] expression of molecular chaperones,[5] and regulation of certain gene expression programs.[6] As is well known, cells respond to damaging stimuli frequently by synthesizing a family of molecular chaperones (heat shock proteins).[7,8] In addition, cells can cope with stress response through microRNAs (miRNAs) to help restore balance upon sudden environmental changes.[9]

The miRNAs, a class of ~22 nucleotide non-coding RNAs, are loaded onto Ago protein to target sites predominantly in the 3′ UTRs of the cognitive mRNAs, resulting in the destabilization of the mRNAs and/or inhibition of translation to regulate many cellular responses.[10,11] As cells can exploit the mechanisms of activation of certain gene expression programs to deal with stress responses, more and more investigations have been conducted to examine the roles of miRNAs in stress responses.[12–16] Several lines of evidence indicate that stress conditions can alter the expression levels of miRNAs.[12–15] Upon DNA damage, p53 can induce the transcriptions of miR-34a, miR-34b, and miR-34c.[12] A tumor suppression factor, miR-34a, can regulate cell cycle, differentiation, apoptosis, and metastasis of cancer cells via controlling the expression of a series of target genes.[17] The delivery of miR-34a mimic becomes a promising strategy of tumor treatment.[17] As reported, the miRNAs of marine invertebrate *Marsupenaeus japonicus* shrimp present different expression patterns in response to virus infection.[13,14] The profile of miRNAs is changed in HIV type 1 (HIV-1) sero-positive individuals.[15] Emerging data have shown that miRNAs play key roles in the regulation of metabolism upon stress responses.[16] When human hepatocytes are challenged with hepatitis C virus, miR-146a-5p can control fatty acid metabolism and energetic metabolism that contribute to the pathogenesis of liver disease.[16] Therefore, the miRNAs functioning in the stress response processes can regulate the metabolism of organisms. It is well known that tumorigenesis is associated with the metabolic disturbance. Previous study has demonstrated that the altered cellular metabolism in cancer can result in malignant transformation and the initiation, growth, and maintenance of tumors.[18] In this context, miRNAs may bridge the stress response and tumor progression. The miRNAs possessing antiviral activity may have antitumor capacity. However, this issue has not been explored.

To address this concern, the effects of shrimp miR-34 on tumorigenesis of breast cancer were investigated in the present study. Shrimp

Received 5 July 2017; accepted 22 October 2017;
https://doi.org/10.1016/j.omtn.2017.10.016.

Correspondence: Xiaobo Zhang, Zhejiang University, College of Life Sciences, 866 Yuhangtang Road, Room 418, Hangzhou 310058, The People's Republic of China.
E-mail: zxb0812@zju.edu.cn

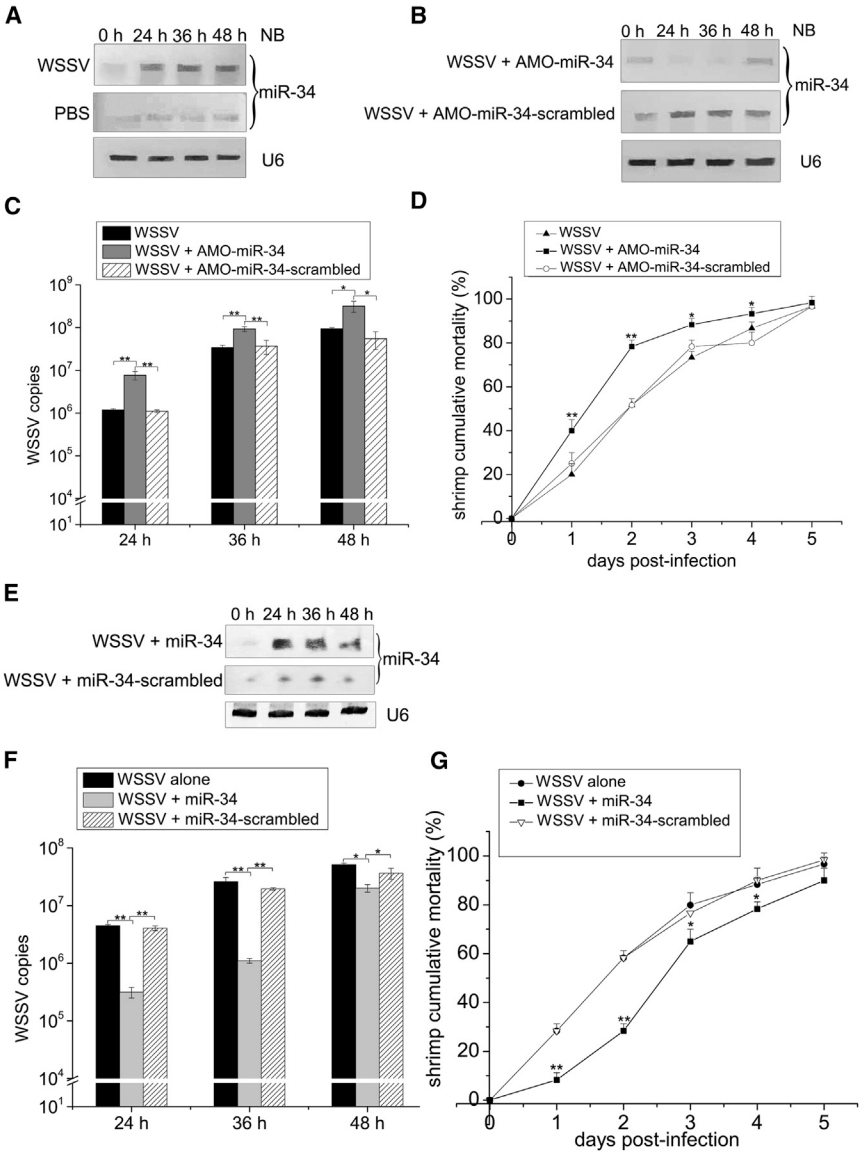

Figure 1. Antiviral Activity of Shrimp miR-34 in Shrimp

(A) The expression profile of shrimp miR-34 in WSSV-challenged shrimp. Shrimp were infected with WSSV. As a control, PBS was included in the injection. At different times post-infection, shrimp were subjected to northern blot analysis (NB) to evaluate the level of miR-34. The numbers represent the time points after WSSV infection in the time course assays. U6 was used as a control. The treatments are shown on the left and the probes are indicated on the right. (B) The detection of shrimp miR-34 expression in miR-34-silenced shrimp. Shrimp were co-injected with WSSV and AMO-miR-34. AMO-miR-34-scrambled was included in the injection as a control. At various times after injection, shrimp were collected for northern blot analysis (NB) to evaluate the level of miR-34. (C) The influence of shrimp miR-34 silencing on virus copy number. The WSSV copy number in virus-challenged and miR-34-silenced shrimp was quantified by real-time qPCR at different times post-infection. (D) The effects of shrimp miR-34 silencing on WSSV-infected shrimp mortality. The numbers on the horizontal axis indicate the post-infection days. (E) The overexpression of miR-34 in shrimp. Shrimp were simultaneously injected with WSSV and shrimp miR-34. As a control, miR-34-scrambled was included in the injection. At different times post-infection, shrimp hemolymph was subjected to northern blotting. U6 was used as a control. The numbers indicate the time points post-infection. The probes are shown on the right. (F) The detection of WSSV copy number in miR-34-overexpressing shrimp by real-time qPCR. (G) Shrimp mortality assays. The treatments are shown at the top. The numbers on the horizontal axis indicate the post-infection days. Statistically significant differences between treatments are indicated with asterisks (error bar, SD; *$p < 0.05$ and **$p < 0.01$).

miR-34, highly homologous to human miR-34a, was involved in the white spot syndrome virus (WSSV) infection.[13,14] The results of this study showed that the antiviral shrimp miR-34 could inhibit the breast cancer proliferation and metastasis.

RESULTS

Antiviral Activity of Shrimp miR-34 in Shrimp

To explore the role of shrimp miR-34 in virus infection, shrimp were challenged with WSSV, followed by the detection of miR-34. Northern blot analysis indicated that WSSV invasion significantly increased the expression level of shrimp miR-34 (Figure 1A), suggesting the involvement of miR-34 in the virus infection.

To reveal the influence of miR-34 on virus infection, the expression of shrimp miR-34 was silenced by the injection of AMO-miR-34 (anti-miR-34 oligonucleotide). Northern blots indicated that miR-34 was knocked down by AMO-miR-34 compared with the control (Figure 1B). The reduced expression of miR-34 resulted in a significant increase in WSSV copy number (Figure 1C) and shrimp cumulative mortality (Figure 1D), demonstrating that shrimp miR-34 played a negative role in WSSV infection. To further explore the effects of shrimp miR-34 on virus infection in shrimp, miR-34 was overexpressed in WSSV-infected shrimp (Figure 1E). The overexpression of shrimp miR-34 led to a significant decrease in WSSV copy number (Figure 1F) and shrimp mortality (Figure 1G), indicating that miR-34 took a positive effect on shrimp antiviral immunity.

These findings presented that shrimp miR-34 possessed antiviral activity in shrimp.

Antitumor Activity of Shrimp miR-34 in Breast Cancer Cells

To explore the effects of antiviral shrimp miR-34 on human tumor progression, the synthesized shrimp miR-34, which was highly homologous to the human miR-34a (Figure 2A), was transfected

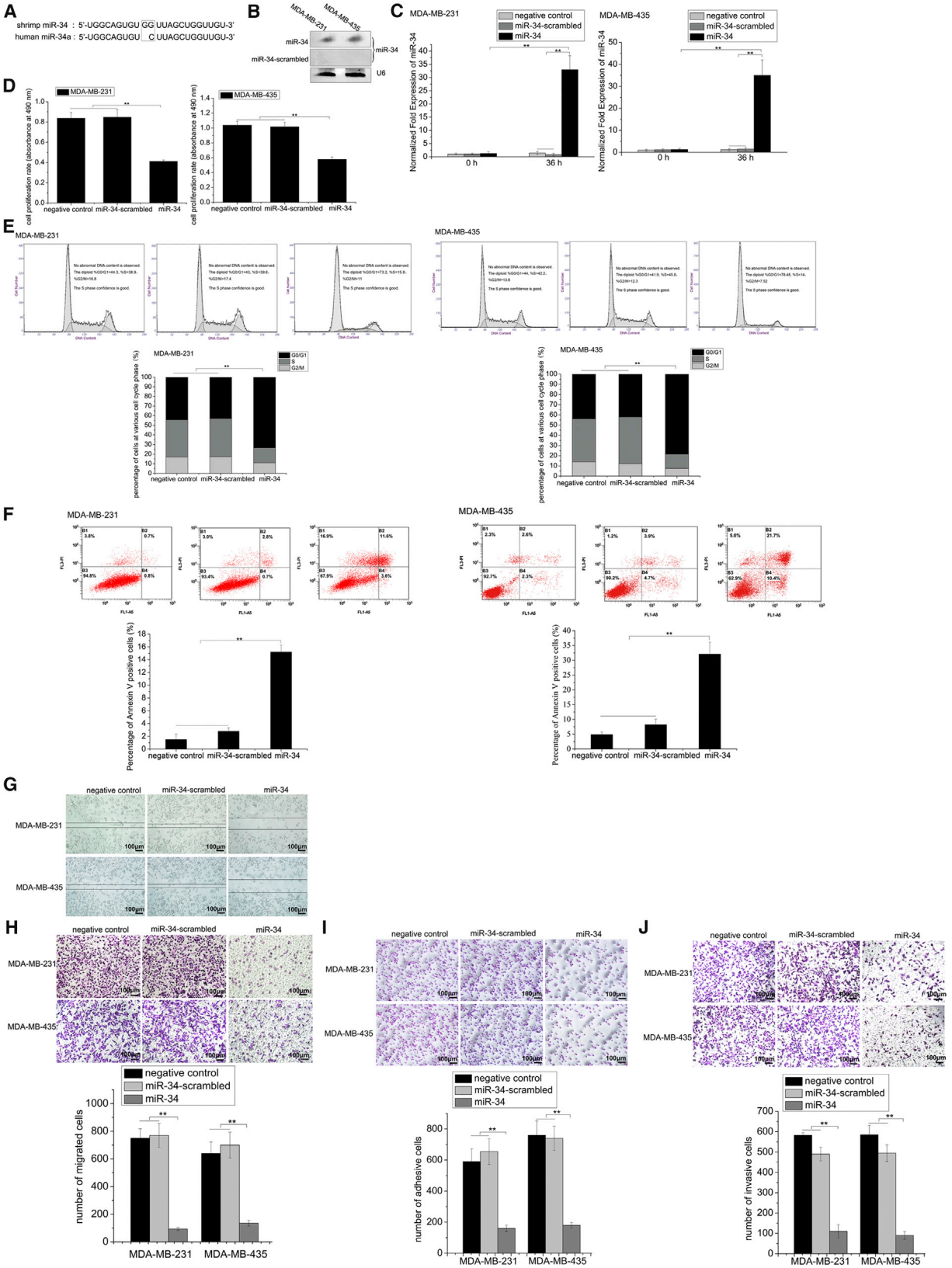

(legend on next page)

into breast cancer cells (MDA-MB-231 and MDA-MB-435), followed by examining the growth and metastasis of cancer cells. Northern blot analysis showed that shrimp miR-34 was expressed in MDA-MB-231 and MDA-MB-435 cells compared to the control (miR-34-scrambled) (Figure 2B). At the same time, real-time qPCR data indicated that, when MDA-MB-231 and MDA-MB-435 cells were transfected with shrimp miR-34, the total levels of miR-34 in breast cancer cells significantly increased compared to controls (negative control and miR-34-scrambled) (Figure 2C). The results demonstrated that the growth of miR-34-expressing cancer cells was significantly inhibited relative to the control (Figure 2D). The effects of shrimp miR-34 on the breast cancer cell cycle were further characterized. Flow cytometry analysis showed that the expression of shrimp miR-34 led to breast cancer cell-cycle arrest at the G0/G1 phase compared with the controls (negative control and miR-34-scrambled) (Figure 2E). Shrimp miR-34 could induce apoptosis of breast cancer cells (Figure 2F). These results indicated that miR-34 played a negative role in cancer cell growth.

To investigate the effect of miR-34 on the breast cancer cell metastasis, miR-34 was transfected into MDA-MB-231 and MDA-MB-435 cells. Interestingly, expression of miR-34 significantly suppressed the migration ability of cancer cells relative to the control (Figure 2G), suggesting the inhibitory role of shrimp miR-34 in breast cancer metastasis. Furthermore, shrimp miR-34 suppressed breast cancer cell metastasis, including cancer cell migration, adhesion, and invasion (Figures 2H–2J).

These findings demonstrated that shrimp miR-34 functioned as a tumor suppressor by inhibiting the growth and metastasis of breast cancer cells.

Underlying Mechanism of Shrimp miR-34 in Inhibiting Breast Cancer Progression

To explore the mechanism by which shrimp miR-34 suppressed breast cancer cell growth and metastasis, target gene prediction was conducted. The results demonstrated that six human genes, which are closely related with cancer cell growth and metastasis (*CCND1* [cyclin D1], *CDK6* [cyclin-dependent kinase 6], *CCNE2* [cyclin E2], *E2F3* [transcription factor E2F3], *MET* [hepatocyte growth factor receptor], and *FOSL1* [Fos-related antigen 1]), were potentially targeted by shrimp miR-34 (Figure 3A), suggesting the involvement of shrimp miR-34 in human tumorigenesis. To characterize the interaction between shrimp miR-34 and its six human target genes, a plasmid containing the 3′ UTR of *CCND1*, *CDK6*, *CCNE2*, *E2F3*, *MET*, or *FOSL1* and synthesized shrimp miR-34 were co-transfected into MDA-MB-231 cells. The luciferase activities of cells co-transfected with miR-34 and the constructed 3′ UTRs of 6 genes were significantly decreased compared with the controls (miR-34-scrambled and the 3′ UTR mutant) (Figure 3B). These data revealed that shrimp miR-34 directly interacted with 6 human target genes (i.e., *CCND1*, *CDK6*, *CCNE2*, *E2F3*, *MET*, and *FOSL1*).

To examine whether the target genes can be regulated by shrimp miR-34 in cells, synthesized shrimp miR-34 was transfected into breast cancer cells and the mRNAs of its 6 target genes were examined. Real-time qPCR demonstrated that the expression of miR-34 led to significant decreases in the mRNAs of its 6 target genes compared with the controls (Figure 3C). Western blot analysis yielded similar results (Figure 3D). These data indicated interactions between shrimp miR-34 and its human targets in cells.

To explore whether shrimp miR-34 could load onto the human Ago2 complex, shrimp miR-34 was incubated with the Ago2 complex. The electrophoretic mobility shift assay (EMSA) results revealed that shrimp miR-34 could bind the human Ago2 complex (Figure 3E). The finding presented that shrimp miR-34 could function in human cells in a cross-phylum manner by loading onto the human Ago2 complex.

As previously reported, CCND1, CDK6, CCNE2, and E2F3 are required for breast cancer proliferation,[19–21] while FOSL1 facilitates breast cancer migration and invasion.[22] MET promotes the proliferation and migration of breast cancer cells.[23]

Taken together, shrimp miR-34 can inhibit the growth and metastasis of breast cancer cells by targeting *CCND1*, *CDK6*, *CCNE2*, *E2F3*, *MET*, and *FOSL1* genes (Figure 3F).

Figure 2. Antitumor Activity of Shrimp miR-34 in Breast Cancer Cells

(A) Sequence alignment of shrimp miR-34 and human miR-34a. (B) The expression of shrimp miR-34 in breast cancer cells. MDA-MB-231 or MDA-MB-435 cells were transfected with miR-34 or miR-34-scrambled. At 36 hr after transfection, the cells were subjected to northern blotting. U6 was used as a control. (C) Quantification of miR-34 in breast cancer cells. MDA-MB-231 or MDA-MB-435 cells were transfected with shrimp miR-34 or miR-34-scrambled. At 36 hr after transfection, the expression level of miR-34 in cells was analyzed by real-time qPCR. Negative control represents the cells without any treatment. (D) The effects of shrimp miR-34 on cancer cell proliferation. The proliferation rates of miR-34-transfected MDA-MB-231 and MDA-MB-435 cells were examined. MiR-34-scrambled and the cells without any treatment (negative control) were used as controls. (E) The influence of shrimp miR-34 on the cell cycle of breast cancer cells. MDA-MB-231 and MDA-MB-435 cells were transfected with the synthesized shrimp miR-34. As controls, the cells without any treatment (negative control) and the cells transfected with miR-34-scrambled were analyzed. At 36 hr after transfection, the cell cycle was examined by flow cytometry. (F) The impact of shrimp miR-34 on apoptosis of cancer cells. The cancer cells were transfected with shrimp miR-34 or miR-34-scrambled. Then 36 hr later, the percentage of apoptotic cancer cells was evaluated by flow cytometry. The cells without any treatment (negative control) were used as controls. (G) The influence of shrimp miR-34 expression on cancer cell metastasis. miR-34-transfected cancer cells were subjected to wound-healing assays to evaluate the migration ability of cancer cells. (H) The effects of shrimp miR-34 on breast cancer cell migration. MDA-MB-231 and MDA-MB-435 cells were transfected with synthesized miR-34 or miR-34-scrambled and further cultured for 36 hr. (I) The effects of shrimp miR-34 expression on breast cancer cell adhesion. As a control, miR-34-scrambled was included in the assay. (J) The role of shrimp miR-34 in breast cancer cell invasion. Scale bar, 100 μm. In all panels, statistically significant differences between treatments are represented with asterisks (error bar, SD; *$p < 0.05$ and **$p < 0.01$).

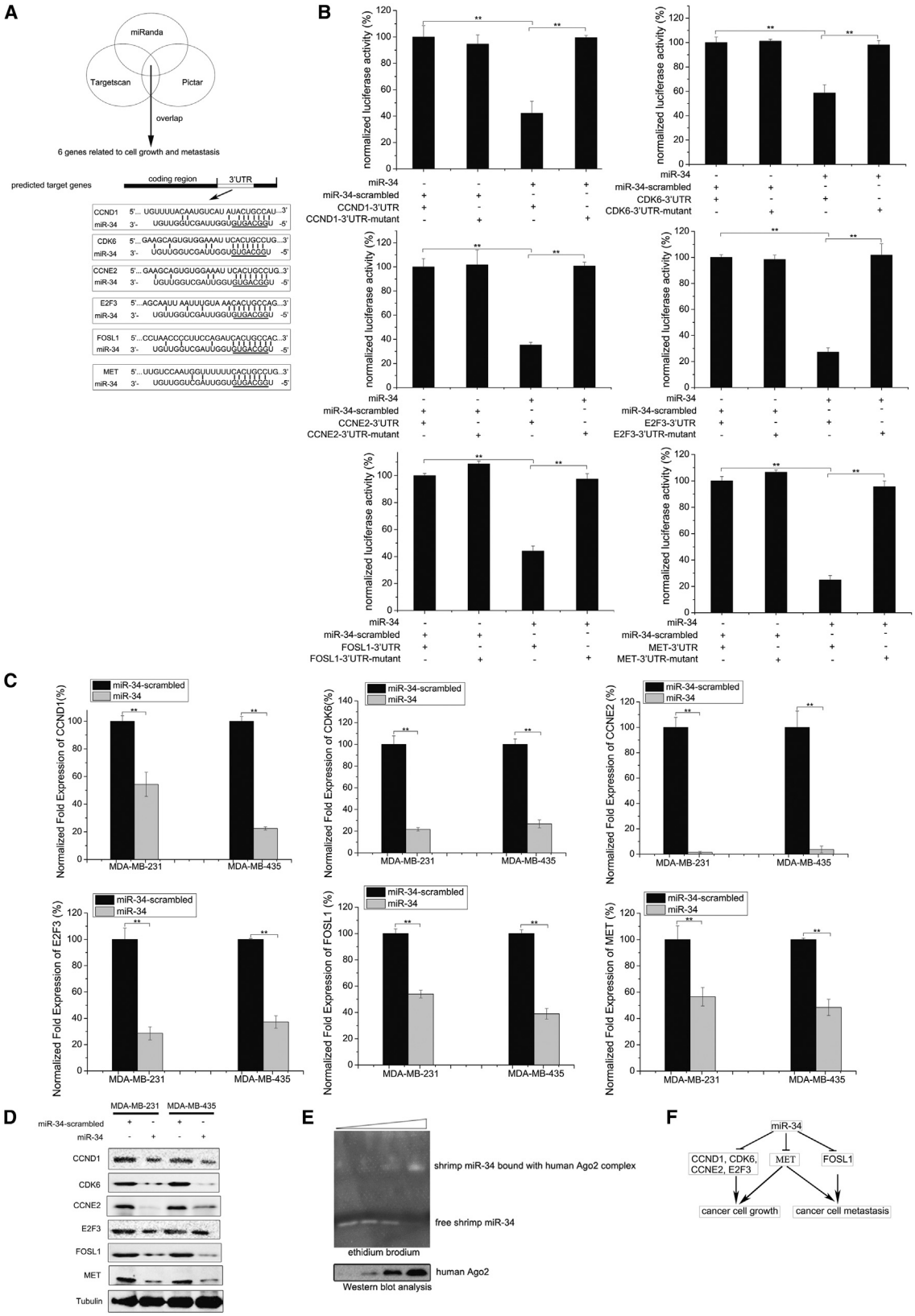

(legend on next page)

Suppression of Breast Tumor Growth and Metastasis by Shrimp miR-34 *In Vivo*

To investigate the effects of shrimp miR-34 on tumorigenesis *in vivo*, MDA-MB-231 breast cancer cells were injected into NOD/SCID female mice, followed by injection with synthesized shrimp miR-34 every 2 days. Tumor growth and tumor metastasis were then examined (Figure 4A).

The tumor growth curve showed that tumor growth was significantly suppressed in mice injected with shrimp miR-34 compared with the control (Figure 4B). No mouse died during the tumor growth experiment. The sizes of the solid tumors in mice injected with shrimp miR-34 were much smaller than those in mice injected with physiological saline (Figure 4C). Real-time qPCR indicated that the expression of shrimp miR-34 in the blood and in the solid tumors of mice injected with miR-34 was significantly elevated relative to the control (Figures 4D and 4E). These data suggested that tumor growth could be inhibited by shrimp miR-34 *in vivo*.

To evaluate the influence of shrimp miR-34 on the expression of its target genes, the expression levels of *CCND1*, *CDK6*, *CCNE2*, *E2F3*, and *MET* were examined. Real-time qPCR, western blot analysis, and immunohistochemistry revealed that miR-34 significantly downregulated the expression of its targets in the solid tumors of mice injected with shrimp miR-34 relative to the control (Figures 4F–4H). To explore whether shrimp miR-34 intravenously injected into mice could load onto human Ago2 complex, Ago2 complex derived from tumor cells was immunoprecipitated, followed by detection of shrimp miR-34. Real-time qPCR demonstrated that the expression level of shrimp miR-34 was much higher in human Ago2 complex from tumor cells treated with miR-34 compared with that of control (Figure 4I), indicating that shrimp miR-34 could load onto human Ago2 complex. These findings indicated that shrimp miR-34 suppressed the growth of breast cancer cells via targeting *CCND1*, *CDK6*, *CCNE2*, *E2F3*, and *MET in vivo*.

Cell metastasis assays indicated that the metastasis of breast cancer cells to the lungs of mice was significantly suppressed when shrimp miR-34 was delivered to the mice by injecting synthesized shrimp miR-34 (Figure 4J). These data showed that shrimp miR-34 could inhibit tumor metastasis *in vivo*. No animal died in the assays. Furthermore, the metastatic tumor nodules in the lungs of mice injected with physiological saline were much larger than those in miR-34-overexpressing mice (injecting synthesized miR-34) (Figure 4K), indicating that shrimp miR-34 decreased the capacity of cancer cell metastasis in mice. Real-time qPCR showed that the expression of shrimp miR-34 in the blood of mice injected with shrimp miR-34 was significantly higher than the control (physiological saline) (Figure 4L). These results showed that shrimp miR-34 could inhibit breast cancer cell metastasis *in vivo*.

Taken together, these findings revealed that shrimp miR-34 resulting from stress response of shrimp against virus infection could suppress tumorigenesis in mice via targeting human genes, showing that miRNAs from the virus-challenged host might be good candidates for antitumor miRNAs.

DISCUSSION

Viruses can induce the metabolic disorder of their host cells, because they complete their life cycles in host cells. To maximize virus replication and propagation in shrimp, a temporal sequestration of shrimp metabolism is observed when shrimp is infected by infectious hypodermal and hematopoietic necrosis virus.[24] In *Drosophila melanogaster*, the cellular processes are disrupted by infection of *Drosophila* C virus (DCV), leading to a decreased metabolic rate in the fruit fly.[25] To deal with the metabolic disorder caused by virus infection, the regulation of gene expression becomes very important for the host to defend against virus invasion. It is well known that miRNAs, important post-transcriptional regulators of gene expression,[10,26] play key roles in virus-host interactions.[27–30] During the host stress response against virus infection, miRNAs can regulate host metabolism by targeting host and/or virus genes.[31] In human hepatoma cells, to inhibit hepatitis C virus replication, miR-27a controls lipid metabolism by targeting the transcription factor of lipid synthesis and many lipid metabolism-related genes that are essential for the production of infectious viral particles.[31] miRNA showing antiviral activity can play vital roles in restoring the metabolic disorder of host cells caused by virus infection.[31] As is well known, tumorigenesis and cancer development result from the metabolic disturbance of cells. Emerging evidence indicates that nearly all cancer types are typical of impaired cellular metabolism.[32] The lipid metabolic disorder in cancer can affect many cellular processes, including cell growth, proliferation, differentiation, and motility.[33] In this context, both virus infection and tumorigenesis are associated with metabolic disturbance of cells. The antiviral miRNAs may have potential antitumor activities by restoring the metabolic disorder of cells. In the present study, the findings demonstrated that shrimp miR-34, a significantly upregulated miRNA in shrimp in response

Figure 3. The Mechanism of Shrimp miR-34 in Inhibiting Breast Cancer Progression

(A) The prediction of genes targeted by shrimp miR-34. The seed sequence of miR-34 is underlined. (B) The direct interaction between shrimp miR-34 and its target genes (i.e., *CCND1*, *CDK6*, *CCNE2*, *E2F3*, *MET*, or *FOSL1*) in breast cancer cells (MDA-MB-231). Luciferase activity was normalized to the ratio of firefly and Renilla luciferase activities. (C) The effects of shrimp miR-34 expression on the expression of miR-34 target genes in breast cancer cells (MDA-MB-231 and MDA-MB-435). (D) The influence of shrimp miR-34 expression on the expression of miR-34 target gene-encoding proteins in breast cancer cells. Protein levels were detected using western blot analysis. As a control, miR-34-scrambled was included in the transfection. Tubulin was used as a loading control. (E) The loading of shrimp miR-34 onto the human Ago2 complex. Shrimp miR-34 was incubated with the human Ago2 complex, followed by EMSA. Shrimp miR-34 was visualized by ethidium bromide staining (top). Human Ago2 protein was detected with western blot analysis (bottom). The wedge indicates the concentration gradient of human Ago2 complex. (F) A model for the role of miR-34-mediated cancer cell growth and metastasis. In all panels, statistically significant differences between treatments are represented with asterisks (error bar, SD; $^{*}p < 0.05$ and $^{**}p < 0.01$).

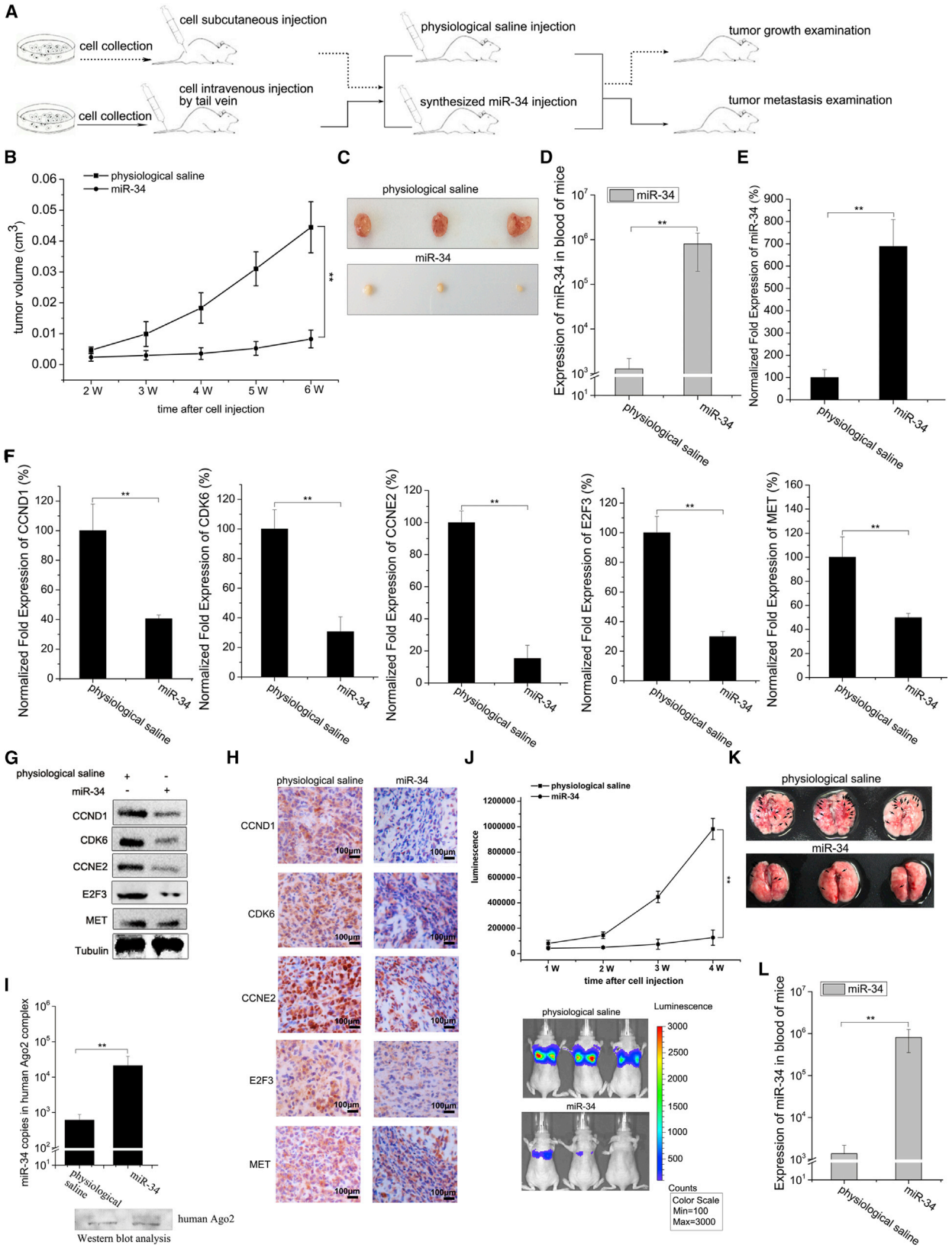

(legend on next page)

to virus infection, played an antiviral role in virus infection and took an antitumor effect on tumorigenesis of breast cancer. Therefore, antiviral miRNAs might serve as good candidates for antitumor drugs.

Shrimp, a kind of crustacean invertebrate, completely depend on the innate immune system to resist virus invasion, because of the lack of acquired immune response system. Invertebrates including shrimp have extended the mechanism of phagocytosis and apoptosis to defend against virus infection in their innate immune response.[34–36] In shrimp, some miRNAs, differentially expressed in the shrimp stress response against virus infection,[13,14] can present their antiviral activities by targeting genes involved in phagocytosis and apoptosis.[37–40] However, whether these antiviral miRNAs are associated with the human cancer progression in a cross-phylum manner still needs to be explored. The results of the present investigation demonstrated that shrimp miR-34, having antiviral capacity in shrimp, could suppress tumorigenesis in humans by loading onto the human Ago2 complex to target CCND1, CDK6, CCNE2, E2F3, FOSL1, and MET genes, which take effects on tumor growth and metastasis.[19–23] In this context, the antiviral miRNAs from virus-challenged shrimp or other invertebrates might be an important source of antitumor drugs in a cross-phylum manner. Although miRNAs can serve as efficient tumor therapeutic agents, the administration of therapeutic miRNA delivery remains to be extensively explored.[41,42] At present, some strategies have been developed to deliver miRNA mimics into xenograft models to inhibit cancer progression.[43,44] Transferrin-conjugated stable nucleic acid lipid particles (SNALPs) encapsulating 2′-O-methylated miR-34a can increase the survival of tumor xenograft mice by specifically targeting the cells overexpressing transferrin receptors.[43] When miR-34a mimic encapsulated in SNALPs is delivered into tumor xenograft mice, a significant tumor growth inhibition and a prolonged mice survival are observed.[44] These strategies can reduce the instability of miRNA mimics in serum.

MATERIALS AND METHODS

Shrimp Culture and WSSV Infection

The culture of *Marsupenaeus japonicus* shrimp and the infection with WSSV were conducted as previously described.[45] Briefly, shrimp were cultured in air-pumped circulating seawater at 25°C. Each treatment comprised 20 individuals in all shrimp experiments. Virus-free shrimp were infected with WSSV (10^5 virus copies/mL) by intramuscular injection. At various time points post-infection, shrimp hemolymph was collected for later use.

Northern Blot Analysis

Total RNA was extracted from shrimp hemocytes or human cells using a mirVanaPTMP miRNA Isolation Kit according to the manufacturer's instructions (Ambion, USA). The extracted RNAs were separated on a denaturing 15% polyacrylamide gel using 1× TBE buffer (90 mM Tris-boric acid and 2 mM EDTA [pH 8.0]), followed by transferring to a nylon membrane (Amersham Biosciences, UK). After UV cross-linking, the membrane was hybridized with a digoxin (DIG)-labeled DNA probe. Signal detection was subsequently conducted using the DIG High Prime DNA Labeling and Detection Starter Kit II (Roche, Germany).

Silencing and Overexpression of Shrimp miR-34 in Shrimp

The expression of shrimp miR-34 was silenced using an anti-miRNA oligonucleotide (AMO). Approximately 15 μg/shrimp of AMO-miR-34 or AMO-miR-34-scrambled was injected into virus-free shrimp by intramuscular injection. The shrimp were simultaneously infected with WSSV (10^5 virus copies/mL). The AMO-miR-34 sequence was 5′-GCTAACCACACTGCCA-3′. As a control, the AMO-miR-34 sequence was randomly scrambled, generating AMO-miR-34-scrambled (5′-ATGCGATGTCAGATAG-3′). AMOs were synthesized with a phosphorothioate backbone and a 2′-O-methyl modification at nucleotides 2 and 8 (Sangon Biotech, Shanghai, China).

To overexpress shrimp miR-34, virus-free shrimp were co-injected with WSSV (10^5 virus copies/mL) and 30 μg/shrimp of synthesized miR-34 (5′-UGGC AGUGUGGUUAGCUGGUUGU-3′ and 5′-ACA ACCAGCUAACCACACUGCCA-3′) or the control miR-34-scrambled (5′-AUUUGACAGAUGCCUAGUACCAG-3′ and 5′-CUGGU ACUAGGCAUCUGUCAAAU-3′). The miR-34 and miR-34-scrambled were synthesized by Shanghai GenePharma (Shanghai, China).

At different time points after injection with the AMOs or miR-34, shrimp hemolymph was collected and stored for later use.

Figure 4. The Suppression of Breast Tumor Growth and Metastasis by Shrimp miR-34 *In Vivo*

(A) A flow chart of the *in vivo* experiments. Tumor growth and metastasis were examined weekly. (B) Tumor growth curves in mice subjected to different treatments. (C) Sizes of the solid tumors in mice subjected to different treatments. Tumors were harvested 6 weeks after injection. (D) The expression level of miR-34 in the blood of mice. At 6 weeks after injection, the blood of mice subjected to different treatments was analyzed by real-time qPCR to evaluate miR-34 expression. (E) The detection of miR-34 expression in solid tumors of mice subjected to various treatments by real-time qPCR analysis. (F) The expression levels of miR-34 target genes in solid tumors. (G) The expression levels of miR-34 target gene-encoding proteins in solid tumors. Protein levels were detected by western blot analysis. Tubulin was used as a control. (H) Immunohistochemical analysis of miR-34 target gene-encoding proteins in solid tumors. The brown and blue colors represent the proteins and nuclei, respectively. The proteins for the detection are indicated on the left. Scale bar, 100 μm. (I) The loading of shrimp miR-34 onto human Ago2 complex in tumor cells derived from mice. Human Ago2 complex of tumor cells treated with shrimp mR-34 or physiological saline was immunoprecipitated, followed by western blot analysis (bottom). Shrimp miR-34 in human Ago2 complex was detected by real-time qPCR (top). (J) The metastasis of breast cancer cells in mice. The capacity of breast cancer cell metastasis in mice subjected to different treatments was examined weekly after injection. Images showing cancer cell metastasis to the lungs of mice at 4 weeks after injection are shown. (K) Representative images displaying lung tumor nodules in mice subjected to various treatments. (L) Detection of miR-34 expression level in the blood of mice subjected to different treatments using real-time qPCR. Statistically significant differences between treatments are indicated using asterisks (error bar, SD; *$p < 0.05$ and **$p < 0.01$).

Quantification of WSSV Copy

Viral DNA was extracted using a TIANmp Genomic DNA Kit (Tiangen Biotech, Beijing, China) according to the manufacturer's protocols. The viral genomic DNA was then subjected to real-time qPCR using WSSV-specific primers (5′-CCACCAATTCTACTCATGTACC AAA-3′ and 5′-TCCTTGCAATGG GCAAAATC-3′) and a TaqMan probe (5′-FAM-CTGGGTTACGAGTCTAA-TAMRA-3′). The PCR conditions were 95°C for 1 min, followed by 45 cycles at 95°C for 15 s, 52°C for 30 s, and 72°C for 30 s. A linearized plasmid containing a 1,400-bp DNA fragment from the WSSV genome was used as an internal standard.[45]

Shrimp Cumulative Mortality Assay

The shrimp cumulative mortality was monitored daily. The experiments were biologically replicated three times.

Cell Culture

Human breast cancer cell lines (MDA-MB-231 and MDA-MB-435) were purchased from The Cell Bank of Type Culture Collection of Chinese Academy of Sciences, Shanghai, China. MDA-MB-231 and MDA-MB-435 cells were cultured in Leibovitz's L-15 medium (Gibco, USA) supplemented with 10% fetal bovine serum (FBS) at 37°C without CO_2.

Expression of Shrimp miR-34 in Cells

Cells (5×10^5) were cultured overnight and transfected with 20 nM synthetic shrimp miR-34 (5′-UGGCAGUGUGGUUAGCUGGUUGU-3′ and 5′-ACAACCAGCUAA CCACACUGCCA-3′) or miR-34-scrambled (5′-UUCUCCGAA CGUGUCACGUU U-3′ and 5′-AAACGUG ACACGUUCGGAGAA-3′) using Lipofectamine RNAiMAX (Life Technologies, USA). The miRNAs were synthesized by Shanghai GenePharma (Shanghai, China). At 36 hr after transfection, cells were subjected to northern blot analysis to detect the expression level of miR-34.

Cell Proliferation Assay

Cells (1×10^4/well) were plated onto a 96-well plate. After transfection with 20 nM synthetic shrimp miR-34 or miR-34-scrambled using Lipofectamine RNAiMAX (Life Technologies, USA), the cells were cultured for 36 hr. Cell proliferation was monitored using a CellTiter 96 AQueous One Solution Cell Proliferation Assay Kit (Promega, USA), according to the manufacturer's protocol. The cell proliferation rate (absorbance at 490 nm) was examined in an iMARKTM microplate reader (Bio-Rad, USA).

Wound-Healing Assay

When cells reached approximately 70% confluency in a 24-well plate, a 100-μL pipette tip was used to create a linear wound in the confluent monolayer. The cells were then treated with 20 nM synthetic shrimp miR-34 or miR-34-scrambled. After culturing for 36 hr, the cell images were acquired using a Nikon Ti-S microscope (Nikon, USA).

Real-Time qPCR of miR-34 and mRNAs

To examine miR-34 expression in cells, total RNA was extracted with an RNA Isolation Kit (Ambion, USA), according to the manufacturer's instructions. A Reverse Transcription Kit (Applied Biosystems, USA) was used to perform the transcription reaction. Real-time qPCR was conducted using the standard TaqMan Micro-RNA Assay (Applied Biosystems, USA). U6 (Applied Biosystems) was included as an internal control. The $2^{-(\Delta\Delta Ct)}$ method was used to calculate the relative level of miRNA expression. PCR was conducted by incubation at 95°C for 10 min followed by 50 cycles at 95°C for 15 s and 60°C for 1 min.

To assess the miR-34 level in the blood of mice, the synthesized shrimp miR-34 was diluted into gradient concentrations (10^3, 10^4, 10^5, 10^6, 10^7, 10^8, and 10^9/μL). Then the diluted shrimp miR-34 was used as an internal standard. Real-time qPCR was conducted using the standard TaqMan Micro-RNA Assay (Applied Biosystems, USA). PCR was also conducted by incubation at 95°C for 10 min followed by 50 cycles at 95°C for 15 s and 60°C for 1 min.

To assess the mRNA levels of cyclin D1 (CCND1), cyclin-dependent kinase 6 (CDK6), cyclin E2 (CCNE2), transcription factor E2F3, hepatocyte growth factor receptor (MET), and Fos-related antigen 1 (FOSL1), 150 ng extracted RNAs was subjected to real-time qPCR as described above. The human glyceraldehyde-3-phosphate dehydrogenase (GAPDH) gene was used as a control. Sequence-specific primers (CCND1, 5′-CCCTCGGTGTCCTACTTCAAATGT-3′ and 5′-GGAA GCGGTCCAGGTAGTTCAT-3′; CDK6, 5′-AGAGCAAGATAATA AAGGAGATGGG-3′ and 5′-CATGTGAGACTTTGAGTAGACCT GA-3′; CCNE2, 5′-GCATTATGACACCACCGAAGA-3′ and 5′-AG GGCAATCAATC ACAGCAC-3′; E2F3, 5′-TGACTGCGTGA GCC TTAGAA-3′ and 5′-CAAGAGC CACAACAAAG AACAG-3′; FOSL1, 5′-CCAACTCCAGCAACTTCTTCT-3′ and 5′-CTCTGGCA CAAATGGGAAA-3′; MET, 5′-CTCTACTTTCATTGGGGAGCA-3′ and 5′-CCT CATCATCAGCGTTATCTTC-3′; and GAPDH, 5′-GGTATCGTGGAAGGACTCATGA C-3′ and 5′-ATGCCAGTGAG CTTCCCGTTCAG-3′) were synthesized.

Cell Cycle Assay

To examine the cell cycle, fluorescence-activated cell sorting (FACS) analysis was performed. Cells (4×10^5) were plated onto a 25-cm^2 culture flask and then transfected with 20 nM synthesized double-stranded shrimp miR-34 (5′-UGGCAGUGUGGU UAGCUGGU UGU-3′) or miR-34-scrambled (5′-UUCUCCGAACGUGUCA CGUU U-3′) using Lipofectamine RNAiMAX (Life Technologies, USA). The miRNAs were synthesized by Shanghai GenePharma. At 36 hr after transfection, the cells were collected and fixed with 70% ethanol at −20°C overnight. After centrifugation at 300 × *g* for 10 min, the cells were resuspended in PBS. The cells were then incubated with RNaseA (200 μg/mL, Sangon Biotech, China) for 30 min at 37°C and stained with propidium iodide (PI) solution (20 μg/mL, Sigma-Aldrich, USA) for 15 min at 37°C. The cells were examined using a FACSCalibur flow cytometer (BD Biosciences, USA). Cell Quest Pro software (BD Biosciences, USA) was used to analyze the flow cytometry data.

Apoptosis Detection with Annexin V

Apoptosis assay was conducted using a fluorescein isothiocyanate (FITC) Annexin V apoptosis detection kit I (Becton Dickinson, USA), according to the manufacturer's protocol. Cells were harvested and washed by cold PBS. Then the cells were resuspended in 1× annexin binding buffer. Alexa Fluor488 Annexin V and PI were subsequently added to the cells. After incubation at room temperature for 15 min in the dark, the cells were added with 1× annexin binding buffer. The samples were analyzed with a flow cytometer at an excitation of 575 nm.

Cell Migration Assay with the Boyden Chamber

The examination of cancer cell migration was performed using 24-well Boyden chambers with 8-μm inserts (Corning, USA). Cells were transfected with 20 nM synthetic shrimp miR-34 or miR-34-scrambled. Then 36 hr later, the cells were collected and resuspended in serum-free medium. Cells (3×10^4 for MDA-MB-231 and 4×10^4 for MDA-MB-435) were then plated into the inserts. The inserts were placed in wells containing 600 μL 10% serum-containing medium. After incubation for 24 hr, the inserts were carefully washed with PBS three times and fixed with 4% paraformaldehyde (Sigma-Aldrich, USA) for 15 min. The cells were washed with PBS and stained with crystal violet (0.005%, Beyotime Biotechnology, Shanghai, China) for 15 min. The cells on the upper sides of the membranes were wiped with a cotton swab. A Nikon Ti-S microscope (Nikon, USA) was used to acquire images of the migrated cells. The results indicated the number of migrated cells per ×200 field micrograph for each sample well. All experiments were biologically replicated three times.

Cell Adhesion Assay

The cell adhesion assay was conducted to determine the ability of cancer cells to adhere to fibronectin. A 24-well plate was pre-coated with fibronectin (20 μg/mL, Sigma-Aldrich, USA) at 37°C for 2 hr. After washing with PBS, 10% bovine serum albumin (BSA) was added to the wells, followed by incubation at 37°C for 0.5 hr to block non-specific proteins. At the same time, 20 nM synthetic shrimp miR-34 or miR-34-scrambled was transfected into cells. Then 36 hr later, the cells were collected and resuspended in serum-free medium. The cells (5×10^4) were transferred to the pre-coated plate. After culture for 30 min at 37°C, non-adherent cells were removed. The adherent cells were washed twice with PBS and fixed with 4% paraformaldehyde, followed by staining with methylrosanilinium chloride solution (Beyotime Biotechnology, Shanghai, China) for 15 min. The number of stained cells was examined under a microscope.

Cell Invasion Assay

Cells were transfected with 20 nM synthetic shrimp miR-34 or miR-34-scrambled and cultured for 36 hr. The cells were collected and resuspended in 100 μL serum-free medium. Cell invasion ability was assessed using 24-well Matrigel invasion chambers with 8-μm inserts (Corning, USA). The inserts were pre-activated with DMEM (Gibco, USA) for 2 hr at 37°C. Resuspended cells (5×10^4) were then plated into the inserts. The inserts were placed into wells containing 600 μL 10% serum-containing medium. After incubation for 24 hr, the inserts were carefully washed with PBS and fixed with 4% paraformaldehyde (Sigma-Aldrich, USA) for 15 min, followed by staining with crystal violet (0.005%, Beyotime Biotechnology, Shanghai, China) for 15 min. A Nikon Ti-S microscope (Nikon, USA) was used to acquire images of invasive cells. The results indicated the number of invasive cells per ×200 field micrograph for each sample well.

Prediction of Target Genes

Three computational target prediction algorithms, including TargetScan 5.1 (http://www.targetscan.org), miRanda (http://www.microrna.org/), and PicTar (http://pictar.mdc-berlin.de) were used to predict the human genes targeted by an miRNA. Based on the 3′ UTRs of human genes, the overlapping genes predicted by the algorithms were the potential targets of an miRNA.

Western Blot Analysis

Protein samples from shrimp, cells, or solid tumors were analyzed by SDS-PAGE and transferred to a nitrocellulose membrane (Bio-Rad, USA). The membrane was blocked with 5% milk at 4°C overnight, followed by incubation with the indicated primary antibodies at 4°C overnight. Rabbit anti-human CCND1, CDK6, CCNE2, E2F3, FOSL1, and MET antibodies were purchased from Proteintech Group (USA). The membrane was subsequently incubated with horseradish peroxidase (HRP)-conjugated goat anti-Mouse or anti-Rabbit IgG (Sigma-Aldrich, USA) for 2 hr. Proteins were detected using Western Lightning Plus-ECL Oxidizing Reagent Plus (PerkinElmer, USA).

Dual-Luciferase Reporter Assay

To explore the direct interaction between miR-34 and its target genes, the 3′ UTR of *CCND1*, *CDK6*, *CCNE2*, *E2F3*, *MET*, or *FOSL1* was amplified with sequence-specific primers (*CCND1*, 5′-GCAGAGC TCTGACCTGTTTATGAGATG-3′ and 5′-AATCTCGAGGGGTCC ACCATGGCTAA-3′; *CDK6*, 5′-ATAGAGC TCT TTGGCTGTG GTACCAA-3′ and 5′-GCACTCGAGTGGACAGTGATATTTCA-3′; *CCNE2*, 5′-ATAGAGCTCGGAGGCATTATGACA-3′ and 5′-ATAC TCGAGTG CACTAGTCAAG-3′; *E2F3*, 5′-ATCGAGCTCCTGGT ACCATTGAGT-3′ and 5′-AT ACTCGAGACAGATCTACAC GTAC-3′; *FOSL1*, 5′-ATAGAGCTCCCCACCGGTC CAGCT-3′ and 5′-ATTCTCGAGCTGAGCTGTGCGGTT-3′; and *MET*, 5′-ATAGA GCT CCGGATATCAGCGATC-3′ and 5′-AGTCTCGAGGTTTTG GACTCCAAT-3′). The 3′ UTRs were then cloned into the pmirGLO Dual-Luciferase miRNA Target Expression Vector (Promega, USA).

To generate the 3′ UTR mutants, the seed sequences of the 3′ UTRs were randomly mutated by PCR using sequence-specific primers (*CCND1*, 5′-TTTTGTTTTACAATGTCATATCAGATAATGTA-3′ and 5′-A GAAAACTAAAACTAGTACATTATCTGATATG-3′; *CDK6*, 5′- CA AGAAGCAGT GTGGAAATTTGACATATGGGA-3′ and 5′-TCTT ATAAGACTGTGTCCCATATGT CAAATTT-3′; *CCNE2*, 5′-GCCA ATTCACAAGTTAACTCTTAATTCTGA-3′ and 5′-GTTTTAAAA TCAGAATTAAGAGTTAACTTGT-3′; *E2F3*, 5′-AATTAATTTGT AAAACTGTTAAGAATACT-3′ and 5′-AGCTAGAAAGTATTC

TTAACAGTTTT ACAA-3′; *FOSL1*, 5′-ACCCCTTCCAGATAGACT ATACACTCTC-3′ and 5′-TGAT GGAGAGTGTATAGTCTATCTG GAA-3′; and *MET*, 5′-CCAATGGTTTTTTAGTCAT ATGACCT TT-3′ and 5′-CTT TTAAAGGTCATATGACTAAAAAACC-3′) and the mutated 3′ UTRs were cloned into the pmirGLO Dual-Luciferase miRNA Target Expression Vector.

For the dual-luciferase reporter assay, MDA-MB-231 cells (3×10^4) were plated onto a 96-well plate and co-transfected with synthesized shrimp miR-34 (20 nM) or miR-34-scrambled (20 nM) and the constructed 3′ UTRs of the wild-type (100 ng) or mutants (100 ng) per well. At 48 hr after transfection, passive lysis buffer (Promega, USA) was added to rapidly promote cell lysis. The lysate was subsequently used for luciferase activity detection, according to the manufacturer's instructions (Dual-Luciferase Reporter Assay System, Promega, USA).

EMSA

MDA-MB-231 cells were collected and lysed in lysis buffer (20 mM Tris·Cl, 1 mM EDTA, 150 mM NaCl, and 1% Triton X-100 [pH 7.5]). Then the cell lystate was immunoprecipitated using the polyclonal antibody against human Ago2 for 4 hr at 4°C, followed by incubation with protein A-beads (GE Healthcare, USA) for 4 hr at 4°C. After washing with lysis buffer, the Ago2 complex was resuspended with the reaction buffer (0.1 M KCl, 1 mM DTT, 1 mM MgCl2, and 10 mM HEPES [pH 7.6]). To illustrate the interaction between shrimp miR-34 and human Ago2 complex, the Ago2 complex was subjected to gradient dilution. Subsequently, 4 μM shrimp miR-34 was incubated with the Ago2 complex at different concentrations. After incubation in the reaction buffer for 1 hr at 37°C, the mixture was separated on an 8% native polyacrylamide gel at 100 V for 1 hr. The RNA bands were stained by ethidium bromide. The proteins were subjected to western blot analysis.

Mouse Experiment

To evaluate the influence of miR-34 on tumorigenesis *in vivo*, experiments were performed in mice to examine tumor growth and metastasis. To examine tumor growth *in vivo*, 1×10^6 MDA-MB-231 breast cancer cells were subcutaneously injected into 5 four-week-old non-obese diabetic severe combined immunodeficiency (NOD/SCID) female mice. Three days later, the mice were intravenously injected via the tail vein with 200 nM synthesized shrimp miR-34 dissolved in physiological saline or physiological saline alone every 2 days. To evaluate tumor growth, the length (L) and width (W) of the solid tumor were measured weekly on week 2 after injection. Tumor volume was calculated according to the following formula: volume = $0.52 \times L \times W^2$. At week 6 after injection, the mice were sacrificed and their tumor sizes were evaluated.

To examine tumor metastasis *in vivo*, luciferase-expressing MDA-MB-231 cells were constructed by lentiviral packing. Cells (3×10^5) were injected intravenously via the tail vein into 5 nude mice. The mice were treated with synthesized shrimp miR-34 or physiological saline as described above. The metastatic tumors were imaged using the IVIS Spectrum CT Preclinical *In Vivo* Imaging System (PerkinElmer, USA) weekly after treatments. At week 4 after treatment, the mice were sacrificed and the tumors in the lungs were excised for later use.

Immunohistochemical Analysis

The solid tumors were dissected, formalin-fixed, and embedded in paraffin. The paraffin sections were then incubated with primary antibodies against human CCND1, CDK6, CCNE2, E2F3, or MET (Proteintech Group, USA) at 4°C overnight, followed by incubation with HRP-conjugated goat anti-Rabbit IgG (Sigma-Aldrich, USA) for 2 hr at room temperature. The sections were detected with 3,3′-diaminobenzidine (DAB) according to the manufacturer's instructions (Sangon Biotech, Shanghai, China). After staining the cell nucleus with hematoxylin solution, the sections were observed under a microscope (Zeiss).

Statistical Analysis

One-way ANOVA was used to calculate the mean and SDs for triplicate assays. Statistically significant differences between treatments were determined using Student's t test. Differences were considered statistically significant at $p < 0.05$.

AUTHOR CONTRIBUTIONS

X.Z. designed the study. Y.C. and X.Y. performed the experiments. Y.C. and X.Z. analyzed the data and wrote the manuscript. All authors have read and approved the contents of the manuscript and its publication.

CONFLICTS OF INTEREST

No potential conflicts of interest were disclosed.

ACKNOWLEDGMENTS

This work was financially supported by the National Natural Science Foundation of China (31430089) and the China Ocean Mineral Resources R & D Association (DY135-B-04).

REFERENCES

1. Jindal, S., and Young, R.A. (1992). Vaccinia virus infection induces a stress response that leads to association of Hsp70 with viral proteins. J. Virol. *66*, 5357–5362.
2. Collins, P.L., and Hightower, L.E. (1982). Newcastle disease virus stimulates the cellular accumulation of stress (heat shock) mRNAs and proteins. J. Virol. *44*, 703–707.
3. Kültz, D. (2005). Molecular and evolutionary basis of the cellular stress response. Annu. Rev. Physiol. *67*, 225–257.
4. Kroemer, G., Mariño, G., and Levine, B. (2010). Autophagy and the integrated stress response. Mol. Cell *40*, 280–293.
5. Richter, K., Haslbeck, M., and Buchner, J. (2010). The heat shock response: life on the verge of death. Mol. Cell *40*, 253–266.
6. Spriggs, K.A., Bushell, M., and Willis, A.E. (2010). Translational regulation of gene expression during conditions of cell stress. Mol. Cell *40*, 228–237.
7. Lindquist, S. (1986). The heat-shock response. Annu. Rev. Biochem. *55*, 1151–1191.
8. Calderwood, S.K., Murshid, A., and Prince, T. (2009). The shock of aging: molecular chaperones and the heat shock response in longevity and aging–a mini-review. Gerontology *55*, 550–558.

9. Leung, A.K., and Sharp, P.A. (2007). microRNAs: a safeguard against turmoil? Cell *130*, 581–585.
10. Bushati, N., and Cohen, S.M. (2007). microRNA functions. Annu. Rev. Cell Dev. Biol. *23*, 175–205.
11. Bartel, D.P. (2009). MicroRNAs: target recognition and regulatory functions. Cell *136*, 215–233.
12. Leung, A.K., and Sharp, P.A. (2010). MicroRNA functions in stress responses. Mol. Cell *40*, 205–215.
13. Cui, Y., Huang, T., and Zhang, X. (2015). RNA editing of microRNA prevents RNA-induced silencing complex recognition of target mRNA. Open Biol. *5*, 150126.
14. Huang, T., Xu, D., and Zhang, X. (2012). Characterization of host microRNAs that respond to DNA virus infection in a crustacean. BMC Genomics *13*, 159.
15. Houzet, L., Yeung, M.L., de Lame, V., Desai, D., Smith, S.M., and Jeang, K.T. (2008). MicroRNA profile changes in human immunodeficiency virus type 1 (HIV-1) seropositive individuals. Retrovirology *5*, 118.
16. Bandiera, S., Pernot, S., El Saghire, H., Durand, S.C., Thumann, C., Crouchet, E., Ye, T., Fofana, I., Oudot, M.A., Barths, J., et al. (2016). Hepatitis C Virus-Induced Upregulation of MicroRNA miR-146a-5p in Hepatocytes Promotes Viral Infection and Deregulates Metabolic Pathways Associated with Liver Disease Pathogenesis. J. Virol. *90*, 6387–6400.
17. Misso, G., Di Martino, M.T., De Rosa, G., Farooqi, A.A., Lombardi, A., Campani, V., Zarone, M.R., Gullà, A., Tagliaferri, P., Tassone, P., and Caraglia, M. (2014). Mir-34: a new weapon against cancer? Mol. Ther. Nucleic Acids *3*, e194.
18. Hanahan, D., and Weinberg, R.A. (2011). Hallmarks of cancer: the next generation. Cell *144*, 646–674.
19. Ichikawa, T., Sato, F., Terasawa, K., Tsuchiya, S., Toi, M., Tsujimoto, G., and Shimizu, K. (2012). Trastuzumab produces therapeutic actions by upregulating miR-26a and miR-30b in breast cancer cells. PLoS ONE *7*, e31422.
20. Lee, M., Oprea-Ilies, G., and Saavedra, H.I. (2015). Silencing of E2F3 suppresses tumor growth of Her2+ breast cancer cells by restricting mitosis. Oncotarget *6*, 37316–37334.
21. Murad, H., Hawat, M., Ekhtiar, A., AlJapawe, A., Abbas, A., Darwish, H., Sbenati, O., and Ghannam, A. (2016). Induction of G1-phase cell cycle arrest and apoptosis pathway in MDA-MB-231 human breast cancer cells by sulfated polysaccharide extracted from Laurencia papillosa. Cancer Cell Int. *16*, 39.
22. Yang, S., Li, Y., Gao, J., Zhang, T., Li, S., Luo, A., Chen, H., Ding, F., Wang, X., and Liu, Z. (2013). MicroRNA-34 suppresses breast cancer invasion and metastasis by directly targeting Fra-1. Oncogene *32*, 4294–4303.
23. Ebrahim, H.Y., Elsayed, H.E., Mohyeldin, M.M., Akl, M.R., Bhattacharjee, J., Egbert, S., and El Sayed, K.A. (2016). Norstictic Acid Inhibits Breast Cancer Cell Proliferation, Migration, Invasion, and In Vivo Invasive Growth Through Targeting C-Met. Phytother. Res. *30*, 557–566.
24. Galván-Alvarez, D., Mendoza-Cano, F., Hernández-López, J., and Sánchez-Paz, A. (2012). Experimental evidence of metabolic disturbance in the white shrimp Penaeus vannamei induced by the Infectious Hypodermal and Hematopoietic Necrosis Virus (IHHNV). J. Invertebr. Pathol. *111*, 60–67.
25. Arnold, P.A., Johnson, K.N., and White, C.R. (2013). Physiological and metabolic consequences of viral infection in Drosophila melanogaster. J. Exp. Biol. *216*, 3350–3357.
26. Bartel, D.P. (2004). MicroRNAs: genomics, biogenesis, mechanism, and function. Cell *116*, 281–297.
27. Umbach, J.L., Kramer, M.F., Jurak, I., Karnowski, H.W., Coen, D.M., and Cullen, B.R. (2008). MicroRNAs expressed by herpes simplex virus 1 during latent infection regulate viral mRNAs. Nature *454*, 780–783.
28. Lecellier, C.H., Dunoyer, P., Arar, K., Lehmann-Che, J., Eyquem, S., Himber, C., Saïb, A., and Voinnet, O. (2005). A cellular microRNA mediates antiviral defense in human cells. Science *308*, 557–560.
29. Ren, Q., Huang, X., Cui, Y., Sun, J., Wang, W., and Zhang, X. (2017). Two white spot syndrome virus microRNAs target the Dorsal gene to promote virus infection in *Marsupenaeus japonicus* shrimp. J. Virol. *91*, e02261-16.
30. He, Y., Sun, Y., and Zhang, X. (2017). Noncoding miRNAs bridge virus infection and host autophagy in shrimp in vivo. FASEB J. *31*, 2854–2868.
31. Shirasaki, T., Honda, M., Shimakami, T., Horii, R., Yamashita, T., Sakai, Y., Sakai, A., Okada, H., Watanabe, R., Murakami, S., et al. (2013). MicroRNA-27a regulates lipid metabolism and inhibits hepatitis C virus replication in human hepatoma cells. J. Virol. *87*, 5270–5286.
32. DeBerardinis, R.J., and Thompson, C.B. (2012). Cellular metabolism and disease: what do metabolic outliers teach us? Cell *148*, 1132–1144.
33. Santos, C.R., and Schulze, A. (2012). Lipid metabolism in cancer. FEBS J. *279*, 2610–2623.
34. Wu, W., Zong, R., Xu, J., and Zhang, X. (2008). Antiviral phagocytosis is regulated by a novel Rab-dependent complex in shrimp penaeus japonicus. J. Proteome Res. *7*, 424–431.
35. Zhi, B., Tang, W., and Zhang, X. (2011). Enhancement of shrimp antiviral immune response through caspase-dependent apoptosis by small molecules. Mar. Biotechnol. (NY) *13*, 575–583.
36. Liu, W., Han, F., and Zhang, X. (2009). Ran GTPase regulates hemocytic phagocytosis of shrimp by interaction with myosin. J. Proteome Res. *8*, 1198–1206.
37. Shu, L., Li, C., and Zhang, X. (2016). The role of shrimp miR-965 in virus infection. Fish Shellfish Immunol. *54*, 427–434.
38. Liu, C., Wang, J., and Zhang, X. (2014). The involvement of MiR-1-clathrin pathway in the regulation of phagocytosis. PLoS ONE *9*, e98747.
39. Huang, T., Cui, Y., and Zhang, X. (2014). Involvement of viral microRNA in the regulation of antiviral apoptosis in shrimp. J. Virol. *88*, 2544–2554.
40. Yang, L., Yang, G., and Zhang, X. (2014). The miR-100-mediated pathway regulates apoptosis against virus infection in shrimp. Fish Shellfish Immunol. *40*, 146–153.
41. Calin, G.A., Cimmino, A., Fabbri, M., Ferracin, M., Wojcik, S.E., Shimizu, M., Taccioli, C., Zanesi, N., Garzon, R., Aqeilan, R.I., et al. (2008). MiR-15a and miR-16-1 cluster functions in human leukemia. Proc. Natl. Acad. Sci. USA *105*, 5166–5171.
42. Esquela-Kerscher, A., Trang, P., Wiggins, J.F., Patrawala, L., Cheng, A., Ford, L., Weidhaas, J.B., Brown, D., Bader, A.G., and Slack, F.J. (2008). The let-7 microRNA reduces tumor growth in mouse models of lung cancer. Cell Cycle *7*, 759–764.
43. Scognamiglio, I., Di Martino, M.T., Campani, V., Virgilio, A., Galeone, A., Gullà, A., Gallo Cantafio, M.E., Misso, G., Tagliaferri, P., Tassone, P., et al. (2014). Transferrin-conjugated SNALPs encapsulating 2′-O-methylated miR-34a for the treatment of multiple myeloma. BioMed Res. Int. *2014*, 217365.
44. Di Martino, M.T., Campani, V., Misso, G., Gallo Cantafio, M.E., Gullà, A., Foresta, U., Guzzi, P.H., Castellano, M., Grimaldi, A., Gigantino, V., et al. (2014). In vivo activity of miR-34a mimics delivered by stable nucleic acid lipid particles (SNALPs) against multiple myeloma. PLoS ONE *9*, e90005.
45. Huang, T., and Zhang, X. (2012). Functional analysis of a crustacean microRNA in host-virus interactions. J. Virol. *86*, 12997–13004.